

Reference Sound Speed Profile and Related Ray Acoustics of Bay of Bengal for Tomographic Studies

S. Prasanna Kumar, T. V. Ramana Murty, Y. K. Somayajulu, P. V. Chodankar, C. S. Murty
National Institute of Oceanography, Dona Paula, Goa, India

Reference Sound Profile and Related Ray Acoustics of Bay of Bengal for Tomographic Studies

Summary

Using the archived hydrographic data, a climatological mean sound speed profile has been developed for the Bay of Bengal which will serve as an input (reference profile) to acoustic models. This profile is depth limited with the effective acoustic wave guide situated much below the surface as seen by the variation in the conjugate depth. Ray-tracing carried out using range-independent software revealed that acoustic rays with a flat angle of emergence from the source reach the receiver faster than the steep angle ones. This arrival pattern of the rays is attributed to the weak acoustic waveguide nature of the Bay of Bengal. From the ray arrival structure it is seen that the near axial rays present poor resolution (<10 milliseconds) though they are the first arrivals, while purely refracted steep angle rays have a better resolution and an organised arrival pattern. For refracted rays, the travel time span – first arrival to last arrival – for different receiver depths, varied from 93.3 ms to 354.4 ms over a range of 300 km. When the source and the receiver are located near the channel axis, a maximum number of eigenrays reach the receiver, which reduces considerably when the receiver location is shifted (in the vertical) from the channel axis. The intensity of the eigenrays at the receiver showed variation from about -81 dB to -112 dB. The loss associated with the steep angle rays is less compared to the flat angle rays because the steep angle rays sample the upper layer of the ocean (having strong sound speed gradients) more often than other rays. These simulated ray arrival times and their energy level provide a basis for the identification on the measured ray arrival structure during acoustic field experiments.

Referenzprofil der Schallgeschwindigkeit für tomographische Untersuchungen und damit zusammenhängende Strahlenakustik im Golf von Bengalen

Zusammenfassung

Unter Benutzung archivierter hydrographischer Daten wurde für den Golf von Bengalen ein klimatologisches Schallgeschwindigkeitsprofil entwickelt, das als Eingangsgröße (Referenzprofil) für akustische Modelle dient. Dieses Profil

ist tiefenbegrenzt, wobei der effektive akustische Wellenleiter weit unter der Oberfläche liegt, was aus der Veränderung der konjugierten Tiefe hervorgeht. Eine unter Benutzung entfernungsunabhängiger Software durchgeführte Strahlverfolgung zeigt, daß Schallstrahlen mit einem flachen Ausgangswinkel den Empfänger schneller erreichen als solche, die vom Sender unter steilem Winkel ausgesandt werden. Dieses Verhalten der Strahlen wird auf den nur wenig ausgeprägten akustischen Wellenleiter im Golf von Bengalen zurückgeführt. Aus der Struktur der Ankunftszeiten ist zu erkennen, daß nahezu axiale Strahlen nur geringe Auflösung (<10 ms) ergeben, obwohl sie als erste eintreffen, während steile gebrochene Strahlen eine bessere Auflösung und ein systematisches Muster der Ankunftszeiten zeigen. Für die gebrochenen Strahlen über einen Bereich von 300 km reichen die Laufzeiten für verschiedene Empfängertiefen von 93,3 ms bis 354,4 ms. Wenn Schallquelle und Empfänger in der Nähe der Kanalachse liegen, erreicht eine maximale Zahl von Eigenstrahlen den Empfänger, die sich beträchtlich vermindert, wenn die Lage des Empfängers in vertikaler Richtung von der Kanalachse verschoben wird. Die Intensität der Eigenstrahlen beim Empfänger variiert zwischen etwa -81 dB bis 112 dB. Die Verluste bei steilen Strahlen sind geringer als die von flachen Strahlen, da die ersten die obere Schicht des Ozeans mit ihren starken Schallgeschwindigkeitsgradienten häufiger durchqueren als die anderen. Diese simulierten Ankunftszeiten von Strahlen und ihre Energiepegel liefern eine Grundlage für die Identifizierung gemessener Ankunftsstrukturen bei akustischen Feldmessungen.

Un profil de référence pour la vitesse du son et la propagation par rayons dans le Golfe du Bengale destiné à des études tomographiques

Sommaire

A partir de données hydrographiques archivées on a établi un profil climatologique moyen de la vitesse du son dans le Golfe du Bengale en vue de son utilisation comme profil de référence dans des modèles de propagation. Ce profil est limité en profondeur, et le guide d'onde acoustique effectif est situé bien au-dessous de la surface, comme le montrent les variations de la profondeur conjuguée. Un tracé de rayons réalisé à l'aide d'un logiciel indépendant de la portée a révélé que les rayons à faible angle d'émergence atteignent le récepteur plus rapidement que les rayons à angle abrupt. Ce diagramme d'arrivée des rayons est attribué au faible pouvoir de guidage des ondes du Golfe du Bengale. La répartition des arrivées montre que les rayons proches de l'axe pré-

Received 17 January 1992,
accepted 24 February 1993.

S. Prasanna Kumar, T. V. Ramana Murty, Y. K. Somayajulu, P. V. Chodankar, C. S. Murty, National Institute of Oceanography, Dona Paula, Goa 403 004, India.

sentent une faible résolution (<10 ms) mais qu'ils arrivent les premiers, tandis que les rayons à angle abrupt purement réfractés ont une meilleure résolution et un diagramme d'arrivée organisé. Pour les rayons réfractés, l'étendue du temps de parcours – différence entre la première et la dernière arrivée – pour différentes profondeurs du récepteur varie de 93,3 ms à 354,4 ms sur une distance de 300 km. Lorsque l'émetteur et le récepteur sont situés près de l'axe du canal, un nombre maximum de rayons propres atteint le récepteur; ce nombre décroît considérablement lorsque l'on déplace ver-

ticalement le récepteur par rapport à l'axe du canal. Les variations d'intensité des rayons propres, observées sur le récepteur, allaient de -81 dB à -112 dB environ. La perte associée aux rayons à angle abrupt est moins élevée que celle associée aux rayons à angle faible, car les premiers franchissent la couche supérieure de l'océan (où le gradient de vitesse du son est élevé) plus souvent que les autres. Cette simulation des instants d'arrivée des rayons et de leurs niveaux d'énergie peut servir de base pour l'identification de la structure des arrivées de rayons mesurée lors d'expériences sur le terrain.

1. Introduction

Ocean acoustic tomography, the brain-child of Munk and Wunsch [1], is a method for synoptic monitoring of large scale oceanographic features. The basic physics underlying the concept of tomography is simple and deals with refraction of the sound waves as they propagate in the ocean. Ray ducting in the sound channel introduces multipaths connecting a given source and a receiver. The travel time of a sound pulse reaching a receiver is a function of the speed of sound along its path. Thus the sound waves travelling along different paths contain information about the structure of the medium. If these multipath arrivals can be separated, the portions of the medium they pass through can be identified. Having measured the travel times of these acoustic pulses, the temporally evolving oceanic (sound speed and to a first approximation temperature) fields could be reconstructed with appropriate inversion techniques. This concept triggered off a number of investigations towards the development of a full fledged ocean acoustic tomographic system. Spiesberger et al. [2] confirmed that multipath arrivals were stable in time and could be identified using ray theory. Cornuelle et al. [3] described a field experiment conducted in 1981 to map the field of sound speed due to mesoscale eddies. Worcester et al. [4] carried out a reciprocal transmission experiment to determine currents. More recently Spiesberger and Metzger [5] used by basin-scale transmission to map month-to-month changes in the thermocline. In India, tomography studies were initiated during the nineteen eighties and were mostly confined to simulation aspects that require a sophisticated acoustic propagation model. An a priori knowledge of the statistics of the acoustic field for a given region would enable one to fix the sensor locations suitably in order to obtain the maximum information that will lead to the estimation of the oceanic variability. Earlier some attempts were made to study the sound-speed field and its variability for a limited data set in the central Bay of Bengal through empirical eigenfunction analysis [6]. Subsequently an analytical sound speed profile was obtained for the Bay of Bengal [7] which proved to be reasonable

when tested with computed sound speed values. In the present study, the climatological mean acoustic field in the form of a reference sound speed profile for the Bay of Bengal is obtained in order to carry out eigenray computations and thereby to develop a data kernel for use in tomographic inversions.

2. Data

The quasi-synthetic environmental data of Levitus [8] for the Bay of Bengal have been utilised to obtain annual mean values of temperature and salinity at 33 standard depths from the region encompassing Lat. 0.5° – 22.5° N and Long. 79.5° – 100.5° E. Before proceeding to the sound-speed computations, the temperature and salinity fields were analysed.

2.1. Temperature field

The temperature shows that surface waters in the northern Bay of Bengal are cooler by 1°C than those near the equator (Fig. 1 a). The water column between 75–200 m depth shows the presence of warm core eddies in the Bay of Bengal, while a cold core eddy is seen in the Andaman sea (Fig. 1 b). Another noteworthy feature in the thermal field is the occurrence of warm waters in the region of the Andaman sea between 1500–2000 m depth (Fig. 1 c). At 2000 m depth the Andaman sea water is warmer by about 2°C than the adjoining waters of the Bay of Bengal.

2.2. Salinity field

The surface salinity distribution shows the extent of the influence of fresh water discharge into the Bay. If the 34×10^{-3} isohaline could be considered as the demarcation between the fresh water and saline water, it can be clearly seen that the effect of fresh water is felt in the entire Bay except in the southwestern part (south of 7° N, Fig. 2 a). An interesting feature is the intrusion of low salinity waters from the Andaman sea into the eastern Bay (mainly through 10° channel) between 100 m and 250 m depth

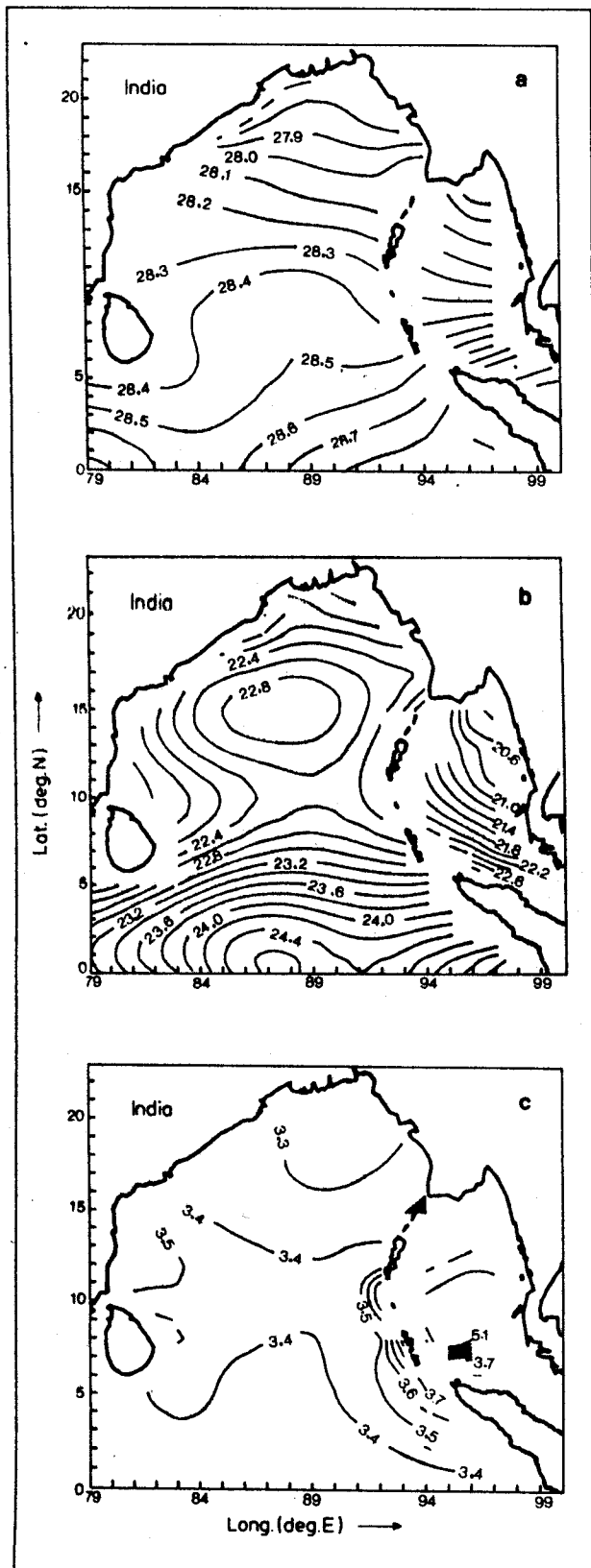


Fig. 1. Temperature distribution at a) the surface, b) 100 m and c) 1750 m depth.

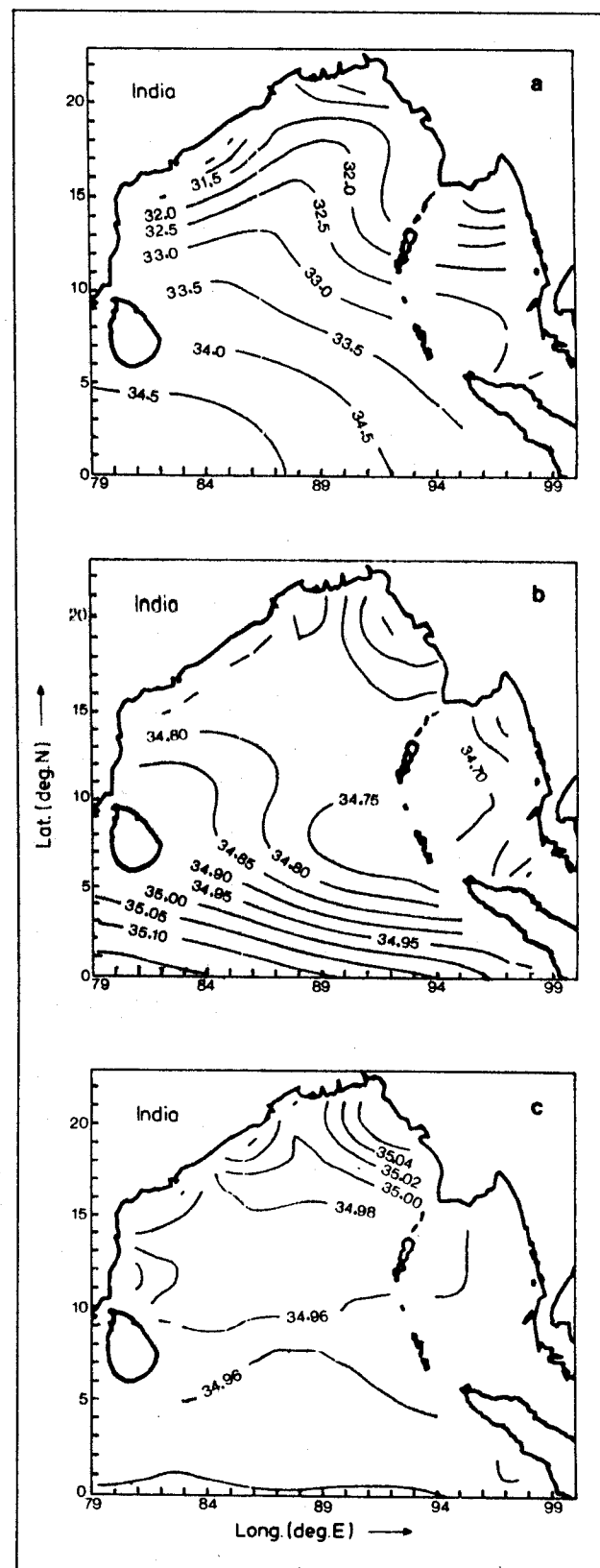


Fig. 2. Salinity distribution at a) the surface, b) 125 m and c) 900 m depth.

(Fig. 2 b). Below this layer down to 1500 m, the waters of the northern Bay, however, exhibit marginally more saline conditions than those of the southern Bay (Fig. 2 c).

3. Method

Having analysed the temperature and salinity fields, sound speeds were computed following the formula of Chen and Millero [9]. From these, a climatological mean sound speed along with the minimum and the maximum values at each of the standard depths, were obtained. This mean profile is used in an acoustic ray-tracing program for the computation of ray parameters such as ray identifier, geometric path, travel time and signal strength.

3.1. Ray-tracing

Ray theory, despite its shortcomings, remains one of the most powerful means to compute sound propagation in a complex environment. It is unique in identifying which part of the ocean is sampled by the sound signal corresponding to the arrival of each pulse. With the aid of modern computers it is easy and economical to simulate measurements prior to the conduct of any field experiment. In view of this, ray theory has been adopted for the present numerical simulation for computing the trajectory of an acoustic signal based on the assumption that (1) the wavelength is much less than the water depth, and (2) the change of sound speed is negligible over several wavelengths.

Following Arthur et al. [10], the ray geometry (Fig. 3) is governed by

$$\frac{dx}{ds} = \cos \theta, \quad \frac{dy}{ds} = \sin \theta$$

$$\frac{d\theta}{ds} = \frac{1}{c} \left[\sin \theta \frac{\partial c}{\partial x} - \cos \theta \frac{\partial c}{\partial y} \right]$$

where θ is the angle of emergence of the sound ray, s is the arc length along the ray, and c is the sound speed. The above equations have been integrated numerically using a Runge-kutta technique for determining the eigenrays.

The acoustic intensity calculations are based on two assumptions: (1) changes in the intensity occur only due to contraction or expansion of the ray tube, and (2) the power transmitted within a ray tube (two adjacent rays separated by 1/100 of a degree) is conserved. The acoustic intensity at any point along the ray path is given by [11]:

$$\text{Intensity} = \frac{I(x)}{I_0} = \frac{\sin \theta_0}{x \cos \theta \cdot \frac{1}{\Delta y / \Delta \theta_0}}$$

where

I_0 = the reference intensity at the source,

θ_0 = the eigenray angle at the source,

θ = the ray angle at the point of measurement,

x = the distance from the source to the point of measurement,

Δy = the vertical distance at the point of measurement between the eigenray and the ray in its immediate vicinity,

$\Delta \theta_0$ = the angle between the eigenray and the ray in its immediate vicinity at the source.

The computed intensity is converted to the practical acoustic unit (decibel dB) by the formula $10 \log(I/I_0)^2$.

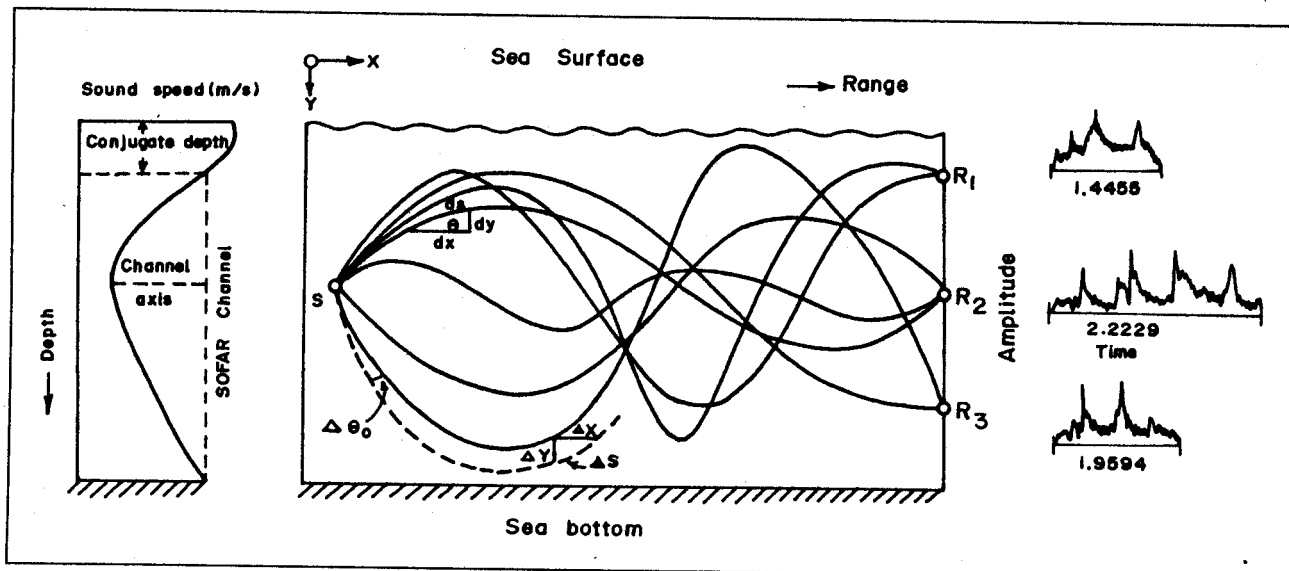


Fig. 3. Schematic presentation of the ray coordinate system. A range of 300 km.

4. Results and discussion

4.1. Sound-speed field

Sound speed at the surface decreases from 1542.5 m/s in the southern Bay to 1536 m/s near the head of the Bay with the contours oriented zonally (Fig. 4 a). This pattern remains down to 75 m, and at 100 m depth (Fig. 4 b) the sound speed values were high near the equator (1535 m/s). In the central Bay another high sound speed cell (1530.5 m/s) is noticed which corresponds to the region of warm water eddy in the thermal field. The waters of the Andaman sea are characterised by a low sound speed compared to those of the Bay of Bengal. In the depth range between 1500 m and 2000 m the magnitudes of the sound speed in the Andaman region are higher compared to the corresponding values in the Bay of Bengal (Fig. 4 c). Below 2000 m depth the variations in sound speed are marginal.

A climatological mean sound speed profile for the Bay of Bengal is presented in Fig. 5 which shows that in the upper 40 m, the sound speed increases with depth, giving rise to a shallow surface duct which is crucial for surface acoustic propagation studies. The deep sound channel axis (SOFAR channel axis) occurs at about 1600 m depth. The marked departure from the mean profile in the depth range between 1500 m–2000 m corresponds to the warm Andaman sea water in that layer.

Considering the importance of the variation of the sound channel parameters such as conjugate depth, axial sound speed, and depth of sound channel axis on the propagation of the acoustic pulses, the spatial distributions of these parameters are presented in Fig. 6. The conjugate depth (depth below the sea surface at which the sound speed equals the near bottom value) varied from 100 m to 300 m (Fig. 6a) due to the variation in bottom topography. This indicates the depth-limited nature of the acoustic profile. As a result, the effective wave-guide lies much below the surface. The depth of the channel axis shows wide spatial variation (Fig. 6 b), with the minimum (1100 m) occurring near the Andaman sea and the northwestern Bay (1200 m), while the maximum of 1730 m occurs in the southwestern and northeastern parts. On average the channel axis in the Bay of Bengal lies at about 1600 m, with sound speeds varying from 1492 m/s to 1493 m/s (Fig. 6c).

4.2. Ray parameters

Acoustic rays were traced using a range-independent software [12] for emergence angles between $+12^\circ$ and -12° at 0.1° intervals. The climatological mean profile (Fig. 5) is used for the ray tracing. A source depth of 1600 m, corresponding to the average depth of the SOFAR channel axis, and receiver depths of 300 m, 500 m, 1000 m, 1500 m, 2000 m over a range of 300 km

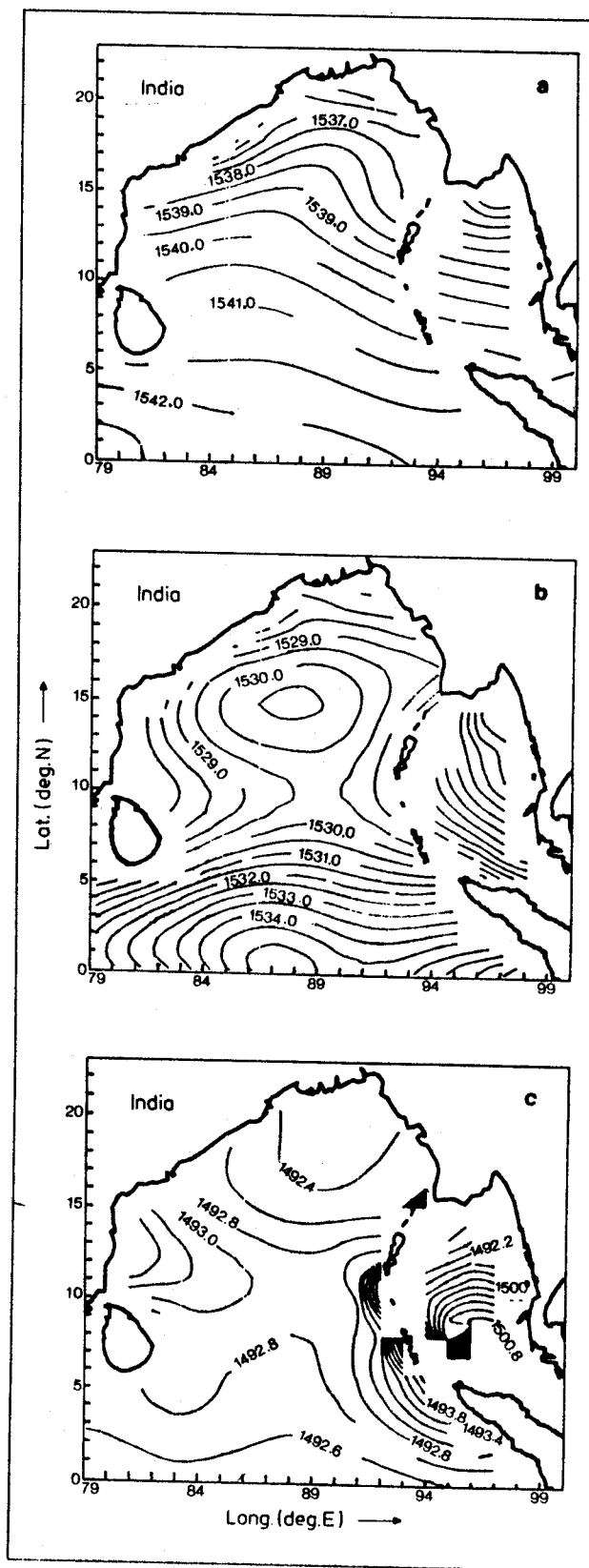


Fig. 4. Sound-speed distribution at a) the surface, b) 100 m and c) 1750 m depth.

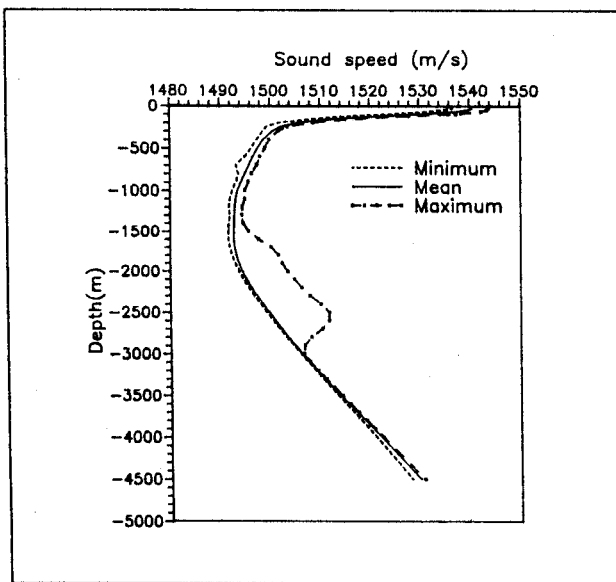


Fig. 5. Climatological mean sound-speed profile for Bay of Bengal.

were selected for computing the eigenrays. The ray parameters obtained from these computations are presented in Table I. The ray identifier (n , RI) in the table, indicates the total number of loops (n), and the number of upper (+) and lower (-) turning points (RI) over the source-receiver range. The ray identifier enables us to identify the rays from their arrival patterns, since the rays usually arrive at the receiver in groups. The travel time span from the first arrival to the last arrival, for different receiver depths, varied from 93.3 ms to 354.4 ms. Another interesting observation is that when the source and the receiver are both located near the channel axis, the number of eigenrays is a maximum (Fig. 7); and as the depth of the receiver is shifted away from the channel axis, the number of eigenrays reduces drastically (Figs. 8 and 9).

A plot of travel time versus launch angle (Fig. 10) gives an idea about the ray arrival structure in the Bay of Bengal. A close examination of the diagram shows that the near-axial rays (-4° to $+4^\circ$) reach the receiver faster than the purely refracted steep angle rays. Further the flat angle rays arrive almost simultaneously, making the travel time resolution (< 10 milliseconds) difficult for ray identification. The rays with launch angles between $> 4^\circ$ to 8° are purely refracted, and have a better travel time spread with a well-defined arrival pattern. However, rays with angles of emergence greater than $+8^\circ$ undergo bottom bounces, seen as kinks in the curve (Fig. 10). This leads to enhanced losses at the bottom boundary. Due to the depth-limited nature of the acoustic profile in the Bay of Bengal, the steep angle rays undergo reflection at the lower boundary and refraction at the upper boundary (RBR), without undergoing surface reflection. The ob-

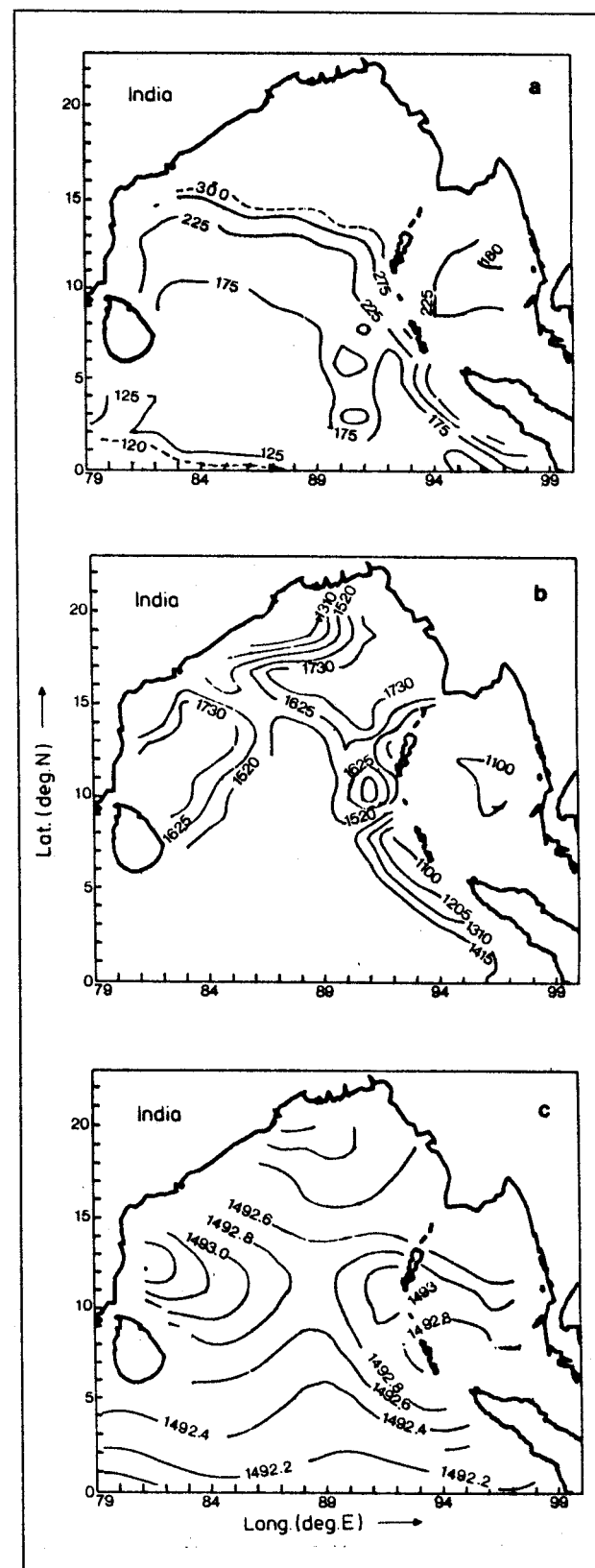


Fig. 6. Spatial distribution of a) conjugate depth, b) depth of sound channel axis and c) axial sound-speed.

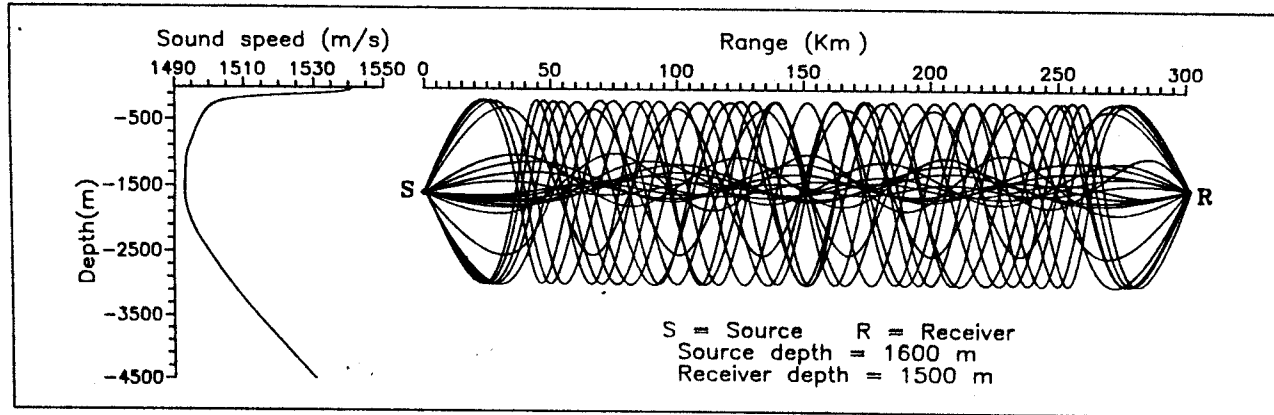


Fig. 7. Eigenrays for a source depth of 1600 m and receiver depth of 1500 m over 300 km range.

Table I. Acoustic ray parameters for source depth = 1600 m and range = 300 km. R_d = receiver depth, n = number of loops, RI = number of upper/lower turning points, θ_0 = launch angle, θ_r = angle at the receiver, ds = path length, T = travel time, dB = unit of intensity.

R_d m	n	RI	θ_0 deg.	θ_r deg.	ds km	T s	-dB
2000	5	(6, -5)	7.8831	-7.394	302.885	202.1888	106.790
	4	(5, -5)	7.5850	7.069	301.670	201.3039	93.307
	4	(5, -4)	6.1231	-5.499	301.151	201.2274	100.734
	4	(4, -5)	-3.4289	2.033	300.483	201.1212	103.523
	4	(4, -5)	-5.4069	4.608	300.888	201.1267	80.971
	5	(6, -5)	7.8553	-7.852	302.751	202.0847	110.795
	4	(5, -4)	5.7774	-5.791	301.033	201.1939	98.547
	4	(4, -4)	1.9243	1.965	300.301	201.1240	106.741
	3	(4, -3)	1.4756	-1.521	300.258	201.1137	105.517
	3	(3, -3)	1.0132	1.081	300.225	201.1039	108.729
1500	3	(3, -3)	0.7102	0.798	300.212	201.1027	108.854
	3	(4, -3)	0.5206	-0.641	300.208	201.1041	110.512
	4	(4, -4)	0.3472	0.512	300.206	201.1062	111.033
	4	(4, -5)	-0.2549	0.453	300.205	201.1066	109.682
	3	(4, -4)	-0.4555	-0.587	300.208	201.1049	110.468
	3	(3, -4)	-0.6355	0.729	300.210	201.1038	109.324
	2	(3, -3)	-0.7510	-0.845	300.211	201.1013	111.284
	2	(3, -3)	-0.9753	-1.052	300.221	201.1014	111.232
	3	(3, -4)	-1.1879	1.249	300.236	201.1067	105.177
	3	(4, -4)	-1.8121	-1.854	300.288	201.1198	105.214
1000	4	(4, -5)	-5.7078	5.722	300.988	201.1579	97.366
	4	(5, -5)	-7.7263	-7.747	301.916	201.4457	111.852
	5	(5, -6)	-7.9203	7.927	302.353	201.7954	107.513
	5	(6, -5)	7.8187	-7.621	302.718	202.0477	97.143
	5	(5, -5)	7.7164	7.534	301.936	201.4893	88.520
	4	(5, -4)	5.5604	-5.282	300.952	201.1612	97.895
	4	(4, -4)	2.2078	1.352	300.336	201.1349	105.12
	4	(4, -5)	-6.1529	5.906	301.135	201.1925	98.537
	4	(5, -5)	-7.4201	-7.171	301.599	201.2851	94.819
	5	(5, -6)	-7.9595	7.769	302.813	202.1157	94.184
500	5	(6, -5)	7.8027	-6.272	302.449	201.8548	108.104
	5	(5, -5)	7.7464	6.358	302.269	201.7265	92.436
	4	(5, -4)	5.3665	-2.736	300.885	201.1357	96.869
	4	(4, -4)	4.5520	0.013	300.698	201.1342	94.472
	4	(4, -5)	-6.4335	4.594	301.239	201.2230	93.934
	4	(5, -5)	-7.0472	-5.314	301.447	201.2475	91.180
300	4	(4, -5)	-6.7190	3.434	301.333	201.2316	90.325
	4	(5, -5)	-6.9237	-3.510	301.399	201.2363	94.877
	6	(6, -7)	-8.7647	6.734	303.790	202.8186	98.953
	6	(7, -7)	-8.8322	-6.675	303.569	202.6612	92.512

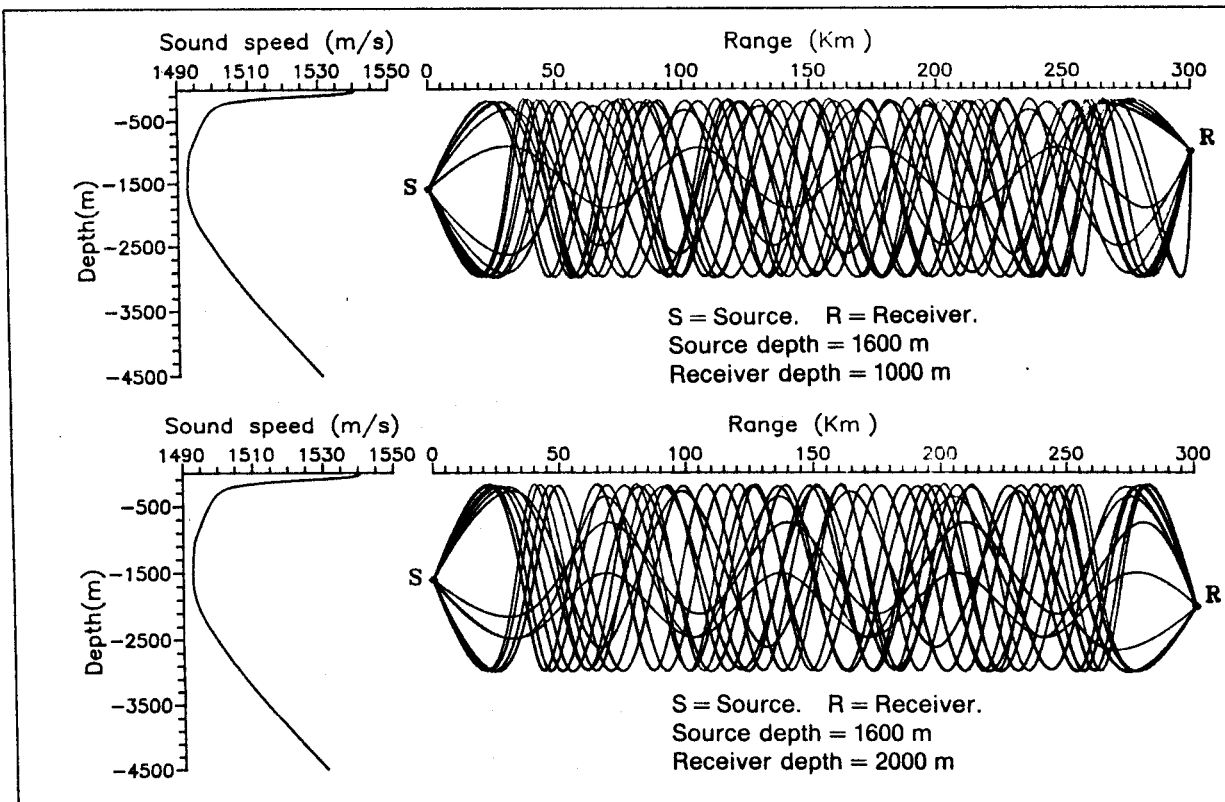


Fig. 8. Eigenrays for a source depth of 1600 m and receiver depth of 1000 m and 2000 m over a range of 300 km.

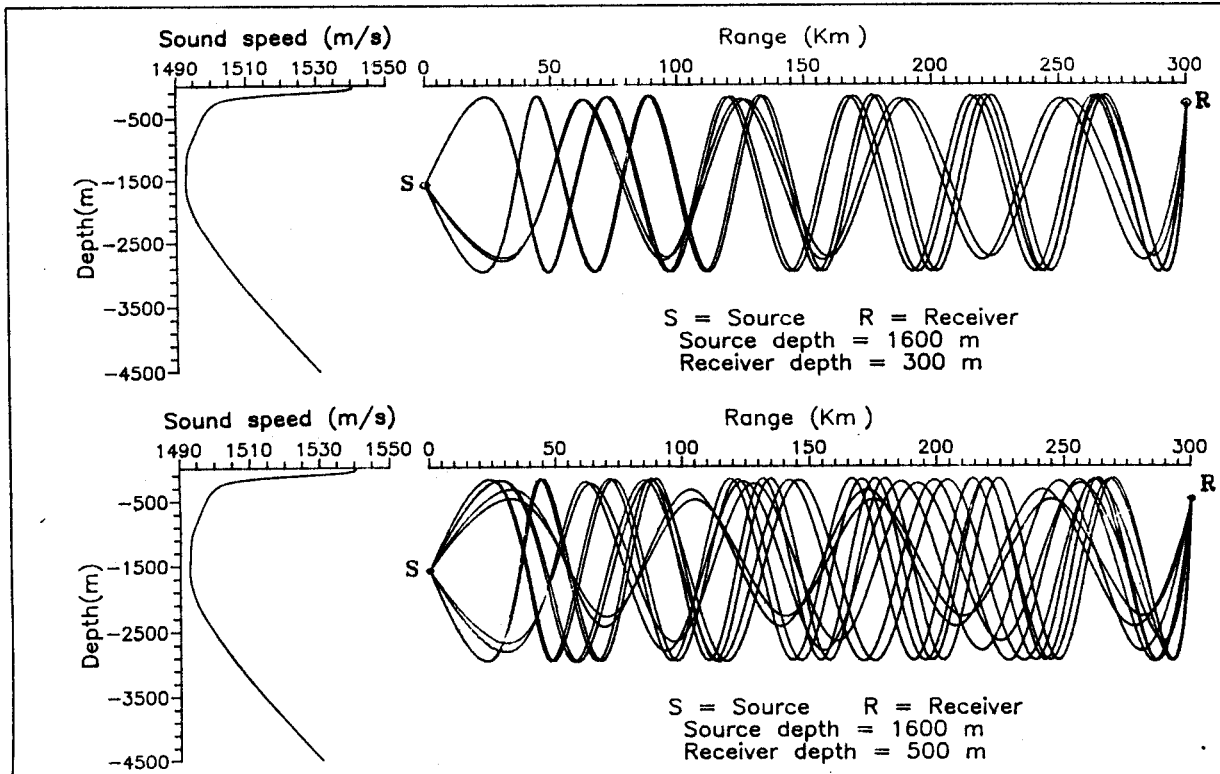


Fig. 9. Eigenrays for a source depth of 1600 m and receiver depth of 300 m and 500 m over a range of 300 km.

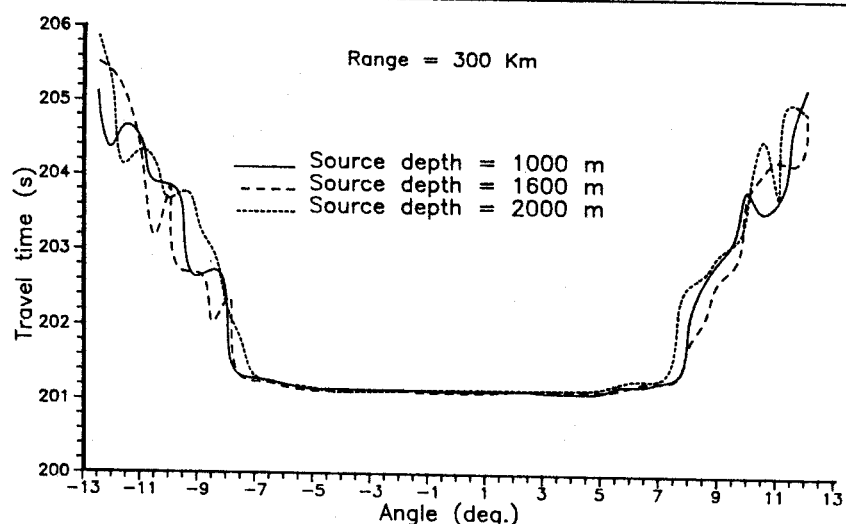


Fig. 10. Angle versus travel time for source located at 1000, 1600 and 2000 m over a range of 300 km.

served arrival pattern results from the weak sound speed gradients within the waveguide, which are characteristic of the Bay of Bengal profile.

4.3. Acoustic intensity

The acoustic intensity was computed for all the eigenrays for different source-receiver configurations (Table I). Figs. 11 and 12 depict the intensity along the ray path for typical eigenrays. In general, the intensity reduces drastically within the first 30 km from the source. The acoustic intensity falls about 60 dB in the first km from the source (spherical spreading), and by about -38 dB within 30 km. Beyond this range the fall in intensity is gradual. The intensity varied from one eigenray to the next. For

example, the intensity for the 7.88° and -3.42° eigenrays (receiver depth 2000 m) varied between -70 dB and -90 dB. However, the variation of intensity over a 300 km range maintained a constant value of about 20 dB, irrespective of the emergence angle and the depth of the receiver. It is also evident that the steep angle rays suffer less loss compared to flat rays, since these rays sample the upper layers of the ocean, having larger sound speed gradients, more often than the flat angle rays. Greater refraction of the steep angle rays results in less loss of energy. In general, the loss at the receiver varied from -81 dB to about -112 dB (Table I). The intensity versus travel time bar graphs (Figs. 13 and 14) show that the travel time resolution associated with the eigenrays is good and their intensity levels at the receiver are adequate for a tomographic study.

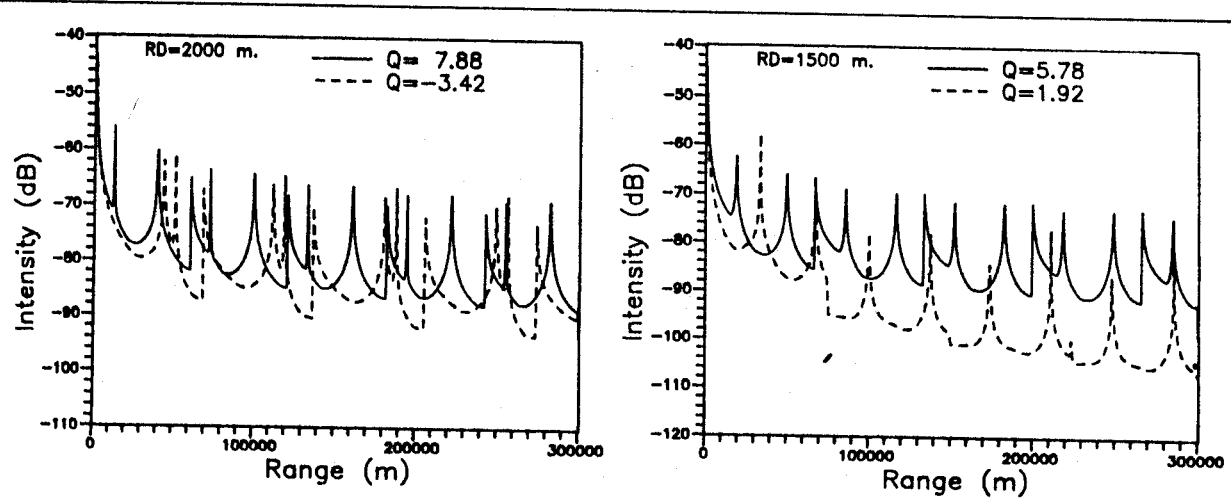


Fig. 11. Intensity along typical eigenrays for receiver depth of 2000 m and 1500 m.

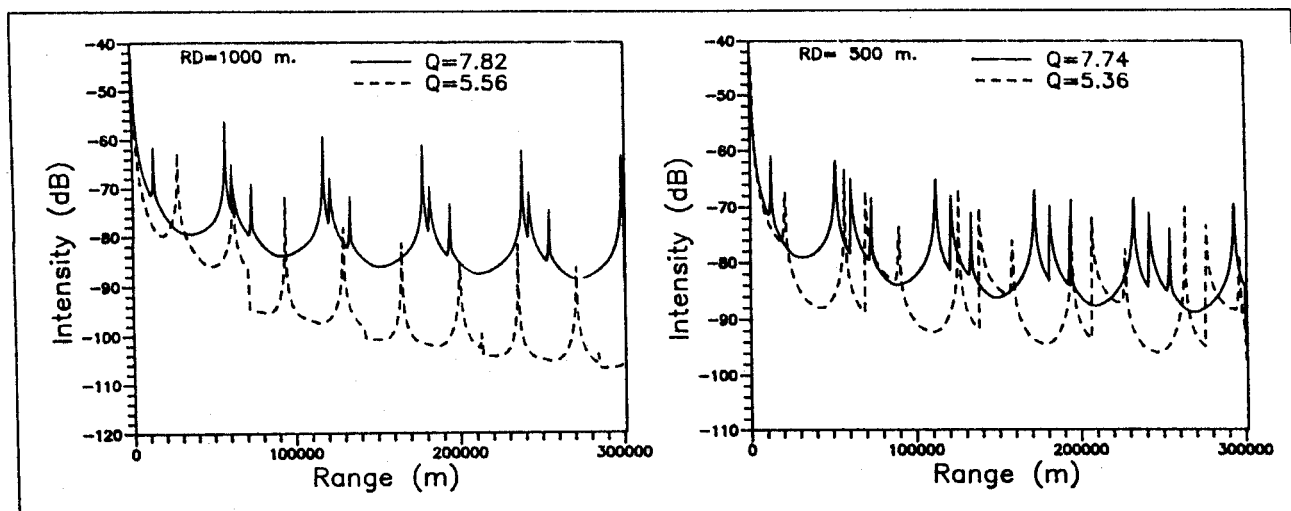


Fig. 12. Intensity along typical eigenrays for receiver depth of 1000 m and 500 m.

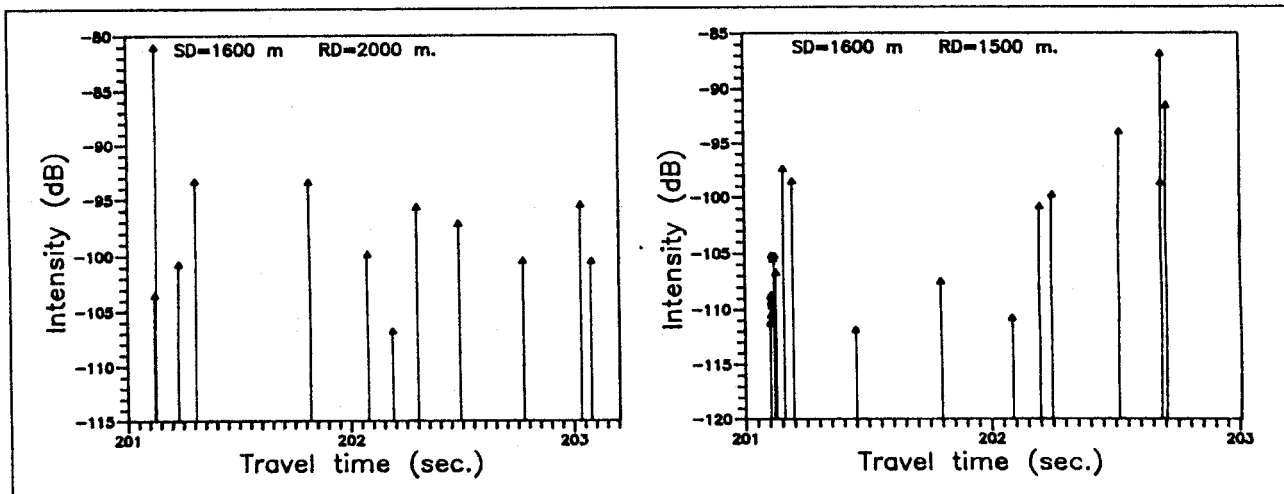


Fig. 13. Bar graph of travel time versus intensity at receiver 2000 m and 1500 m depths.

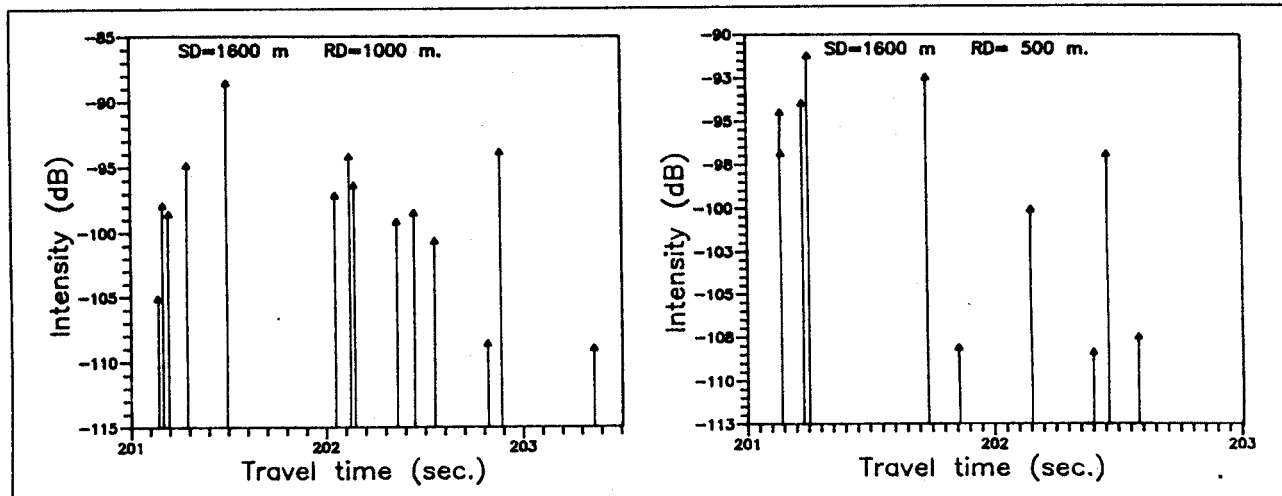


Fig. 14. Bar graph of travel time versus intensity at receiver 1000 m and 500 m depths.

Acknowledgements

The authors are thankful to Dr. B. N. Desai, Director and Dr. J. S. Sastry, Deputy Director, National Institute of Oceanography for their keen interest in this study and to the Department of Ocean Development, Govt. of India for providing the funds.

References

- [1] Munk, W. H., Wunsch, C., Ocean acoustic tomography: A new scheme for large scale monitoring. *Deep-Sea Res.* **26** [1979], 123–161.
- [2] Spiesberger, J. L., Spindel, R. C., Metzger, K., Stability and identification of ocean acoustic multipaths. *J. Acoust. Soc. Amer.* **67** [1980], 2011–2017.
- [3] Cornuelle, B. C., Wunsch, C., Behringer, D., Birdsall, T., Brown, M., Heinmiller, R., Knox, R., Metzger, K., Munk, W. H., Spiesberger, J., Spindel, R., Webb, D., Worcester, P., Tomographic maps of the ocean mesoscale: Pure acoustic. *J. Phys. Oceanogr.* **22** [1985], 133–152.
- [4] Worcester, P. F., Spindel, R. C., Howe, B. M., Acoustic transmission: Instrumentation for mesoscale monitoring for ocean currents. *IEEE Ocean Engg. OE-10* [1985], 123–137.
- [5] Spiesberger, J. L., Metzger, K., Basin-scale tomography: A new tool for studying weather and climate. *J. Geophys. Res.* **96** [1991], 4869–4889.
- [6] Prasanna Kumar, S., Somayajulu, Y. K., Ramana Murty, T. V., Sastry, J. S., Acoustic variability of central Bay of Bengal for tomography. *Oceanologia* **26** [1988], 81–95.
- [7] Ramana Murty, T. V., Prasanna Kumar, S., Somayajulu, Y. K., Sastry, J. S., De Figueiredo, Rui J. P., Canonical sound speed profile for central Bay of Bengal. *Proc. Indian Acad. Sci. (Earth and Planetary Sciences)* **98** [1989], 255–263.
- [8] Levitus, S., Climatological atlas of the world ocean. NOAA professional paper no. 13, U.S. Govt. printing office, Washington, D.C. 1982, 173 pp.
- [9] Chen, C. T., Millero, F. J., Speed of sound in sea water at higher pressure. *J. Acoust. Soc. Amer.* **60** [1977], 129–135.
- [10] Arthur, R. S., Munk, W. H., Issacs, J. D., The direct construction of wave rays. *Trans. Am. Geophys. Un.* **33** [1952], 855–865.
- [11] Moler, C. B., Solomon, L. P., Use of splines and numerical integration in geometrical acoustics. *J. Acoust. Soc. Amer.* **48** [1970], 739.
- [12] Mahadevan, R., Somayajulu, Y. K., Ramana Murty, T. V., Murty, C. S., Sastry, J. S., Tomographic forward problem: Computational details for preparation of data kernel. NIO Tech. Rept. TR-7, 1989, 22 pp.